JACS
JOURNAL OF THE AMERICAN CHEMICAL SOCIETY

COMMUNICATION

pubs.acs.org/JACS

GaN@ZIF-8: Selective Formation of Gallium Nitride Quantum Dots inside a Zinc Methylimidazolate Framework

Daniel Esken,[†] Stuart Turner,[‡] Christian Wiktor,[†,‡] Suresh Babu Kalidindi,[†] Gustaaf Van Tendeloo,[‡] and Roland A. Fischer*[,†]

[†]Department of Inorganic Chemistry II, Ruhr-University Bochum, 44801 Bochum, Germany

[‡]Electron Microscopy for Materials Science, Department of Physics, University of Antwerp, 2020 Antwerp, Belgium

Supporting Information

ABSTRACT: The microporous zeolitic imidazolate framework [$Zn(MeIM)_2$; ZIF-8; MeIM = imidazolate-2-methyl] was quantitatively loaded with trimethylamine gallane [$(CH_3)_3NGaH_3$]. The obtained inclusion compound [$(CH_3)_3NGaH_3$]@ZIF-8 reveals three precursor molecules per host cavity. Treatment with ammonia selectively yields the caged cyclotrigallazane intermediate $(H_2GaNH_2)_3$@ZIF-8, and further annealing gives GaN@ZIF-8. This new composite material was characterized with FT-IR spectroscopy, solid-state NMR spectroscopy, powder X-ray diffraction, elemental analysis, (scanning) transmission electron microscopy combined with electron energy-loss spectroscopy, photoluminescence (PL) spectroscopy, and N_2 sorption measurements. The data give evidence for the presence of GaN nanoparticles (1−3 nm) embedded in the cavities of ZIF-8, including a blue-shift of the PL emission band caused by the quantum size effect.

Metal−organic frameworks (MOFs)[1] are interesting as designer matrices to support metal nanoparticles (NPs) in composite materials of the type "metals@MOFs" for use in gas storage, catalysis, and chemical sensing.[2−6] Only a few related examples exist of metal oxides embedded inside the cavities of MOFs.[7−9] In contrast to zeolites, mesoporous silica, porous carbon materials, etc., MOFs have not yet been investigated as hosts for compound semiconductor (SC) clusters or NPs [i.e., quantum dots (QDs)]. MOFs exhibit tunable photophysical and -chemical properties,[10] and materials systems "SC@MOF" are attractive targets within this context. Herein we report on the very first synthesis of nitride SC NPs within the bulk of MOF microcrystallites. In particular, ZIF-8 [$Zn(MeIM)_2$, where MeIM = imidazolate-2-methyl][11] was loaded with trimethylamine gallane [$(CH_3)_3NGaH_3$] and further treated with ammonia to finally yield GaN@ZIF-8 (Scheme 1). We chose a microporous zeolitic imidazolate framework as host matrix because it is thermally and chemically exceptionally robust and, in particular, is inert against ammonia. In other words, we specifically selected the precursor chemistry of the SC to be orthogonal to the chemistry of the host matrix in order to avoid collapse of the MOF. GaN was chosen because the photocatalytic properties of GaN/ZnO-based materials have attracted much interest within the context of water splitting by visible light irradiation,[12] and we recently reported on ZnO@ZIF-8.[7]

Chemical vapor infiltration (CVI) of ZIF-8 with the highly volatile precursor [$(CH_3)_3NGaH_3$] (**1**) was performed under static vacuum ($p = 10^{-3}$ mbar) at 277 K for 7 days, leading to the inclusion compound [$(CH_3)_3NGaH_3$]@ZIF-8 (**2**) at the saturated loading level. From elemental and thermogravimetric analysis (TGA) data of **2**, three molecules of **1** per host cavity, or 0.5 mole of **1** per mole of ZIF-8, was deduced (Figure S1). The FT-IR spectrum of **2** (Figure 1) shows several characteristic bands for adsorbed **1**, which are slightly shifted to higher wave numbers as compared to neat **1** ($\nu(CH_3) \approx 2900$ cm^{-1}, $\nu(GaH_3) = 1815$ cm^{-1}). In addition, solid-state ^{1}H-MAS NMR measurements of **2** (Figure S2) confirm the presence of unchanged **1**, as derived from the observed resonances at 2.1 ($(H_3C)_3N$) and 4.3 ppm (H_3Ga) as well as at 48.4 ppm in the ^{13}C-MAS NMR spectrum for the methyl group (Figure S3). Powder X-ray diffraction (PXRD) of **2** reveals an intact ZIF-8 structure after CVI and gives an additional hint for the adsorption of **1** *inside* the bulk of the ZIF-8 microcrystals, as suggested by the strong reduction of the (110) peak intensity at $2\theta = 7.3°$ (Figure S4). This effect is ascribed to an overall change in electron density contrast due to the presence of guest molecules inside the cavities and was first described by Lillerud and co-workers, who loaded MOF-5 with guest molecules to study this phenomenon via PXRD in detail.[13] They discovered that the relative intensity of the first MOF reflection at low 2θ angles is strongly dependent on the amount of guests inside the pores. Similar observations were noted for related adsorbate materials of the general type guest@MOF.[7,14−16]

Reaction of the inclusion compound **2** with gaseous ammonia at ambient temperature (323 K) leads to trimerization of **1** and the selective formation of cyclotrigallazane $(H_2GaNH_2)_3$ inside the pores of ZIF-8, as deduced from spectroscopic data (see discussion below). Elemental analysis of sample **3** points to the presence of exactly one trimer per ZIF-8 cage, which matches with the molecular dimensions of $(H_2GaNH_2)_3$ (7.2 × 7.2 × 3.5 Å)[17] and the van der Waals dimensions of the cage (d_{max} = 11.6 Å).[11] Accordingly, we assign the notation $(H_2GaNH_2)_3$@ZIF-8 for the inclusion compound **3**. The cyclotrigallazane remains inside the pores of the host framework, and there is no loss by desorption during the thermally induced formation under ammonia treatment, since the trimer is too bulky to pass through the ZIF-8 aperture ($d = 3.4$ Å). Therefore, it becomes encapsulated by the ZIF-8 environment. In addition, it is significantly stabilized by the caging effect against further aggregation. In contrast, neat $(H_2GaNH_2)_3$ is only stable at low temperatures (<243 K) and is

Received: July 28, 2011
Published: September 13, 2011

Scheme 1. Conceptual Representation of the Confined Trimerization of $[(CH_3)_3NGaH_3]$ inside ZIF-8 To Selectively Yield Caged $(H_2GaNH_2)_3$ and Finally GaN@ZIF-8

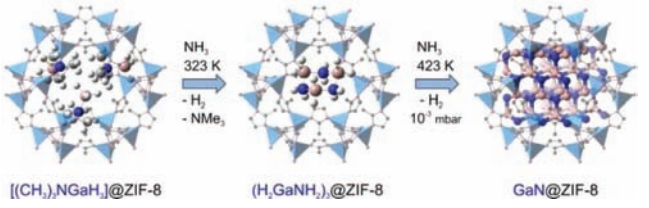

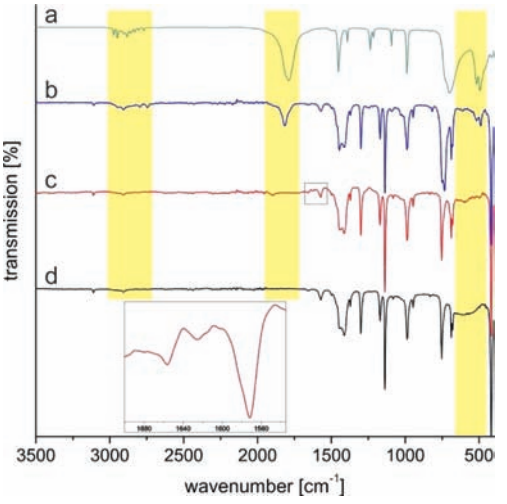

Figure 1. FT-IR spectra of neat trimethylamine gallane (a), $[(CH_3)_3NGaH_3]$@ZIF-8 (b), $(H_2GaNH_2)_3$@ZIF-8 (c), and GaN@ZIF-8 (d).

very prone to react to the thermodynamically more stable product poly(imidogallane) $[(HGaNH)_n]$ by the loss of hydrogen.[18,19] TGA characterization of **3** (Figure S1) shows only a very small weight loss of 2.5% in the temperature range 323−373 K, indicating the release of some remaining traces of NMe_3 as a byproduct of the formation of **3** from **2**. The PXRD pattern of **3** shows the same decrease in intensity of the ZIF-8 (110) reflection, giving again a hint for pore filling, similar to **2** (Figure S4).

^{1}H-MAS NMR measurement of $(H_2GaNH_2)_3$@ZIF-8 (Figure S2) reveals the typical broad ZIF-8 signals (2.2 and 7.3 ppm) and four new signals, which can be assigned to the cyclic trimer as follows: the two close peaks at 1.7 and 1.9 ppm arise from the amido protons of $(H_2GaN\mathit{H}_2)_3$@ZIF-8, emphasizing the chemical nonequivalence of the equatorial and axial H-positions of the cyclic trimer inside ZIF-8. Furthermore, the signals at 5.2 and 6.8 ppm can likewise be traced to the Ga−H bonds **3**.[20] This signal splitting suggests a host−guest interaction possibly involving N···H···N bonds. Additionally, we performed isotope-labeled ^{2}H experiments on encapsulated cyclotrigallazane to measure solid-state ^{2}H NMR (Supporting Information). The reaction of ND_3 with **2** yields $(H_2GaND_2)_3$@ZIF-8 (**3-d$_2$**). Again, two close signals are seen in the ^{2}H NMR experiment, quite similar to the ^{1}H NMR spectrum of the nonlabeled compound, and are assigned to the deuterated amido groups of the cyclic trimer. ^{13}C-MAS NMR measurements of **3** (Figure S4) reveal the typical ZIF-8 shifts, with exception of the signals at 14.4 and 125.6 ppm, exhibiting a small low-field shift

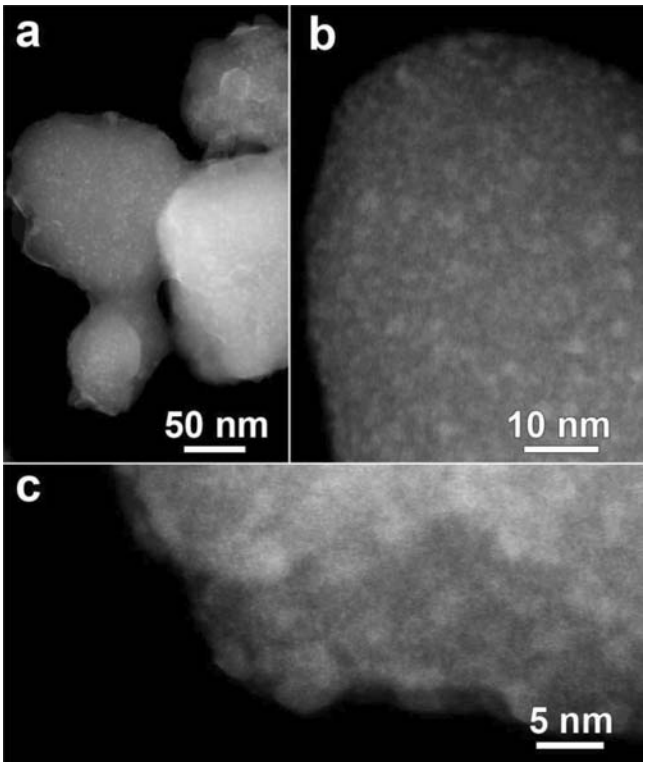

Figure 2. ADF-STEM images of GaN@ZIF-8 (**4**). (a) The ZIF-8 crystals can be seen to be filled with small nanoparticles, imaged as bright dots. (b,c) The smaller NPs exhibit a diameter of ∼1.5 nm and seem to be embedded within the ZIF cavities (1.2 nm size). A bright-field TEM image is given in Figure S9 and shows a speckled contrast induced by the GaN NPs.

in contrast to the activated framework, similar to $[(CH_3)_3NGaH_3]$@ZIF-8.

The FT-IR spectrum (Figure 1) shows the characteristic ν(Ga−H) absorption band of cyclotrigallazane at 1897 cm^{-1}, which is decreased in relative intensity and shifted to higher energies in comparison to **2**. Furthermore, a weak and very broad peak at 580 cm^{-1} becomes visible, which can be assigned to the Ga_3N_3 ring modes.[21] The ν(N−H) stretching vibrations, typically arising between 3200 and 3400 cm^{-1},[22] are too weak to be observed, which might be due to the caging effect. Nevertheless, the scissoring vibration of NH_2 is visible at 1625 cm^{-1}, revealing the presence of amido groups inside the material. The corresponding FT-IR spectrum of the N-deuterated compound **3-d_2** (Figure S7) shows the expected features, the typical absorption bands of the Ga−H and the Ga_3N_3 ring modes and two very weak signals at 2469 and 2435 cm^{-1}, pointing to the ND_2 strechting vibrations of the d_6-trimer.[18]

Further treatment of **3** with ammonia at elevated temperature and pressure (423 K, 3 bar) for 24 h, followed by a thermal annealing step under dynamic vacuum (473 K, 10^{-3} mbar), results in the formation of GaN@ZIF-8 (**4**), with a GaN loading of 13 wt %, as obtained by elemental analysis (0.5 mole of GaN per mole of ZIF-8). The FT-IR spectrum of **4** matches with that of pure, activated ZIF-8 except for a new broad IR absorption band at 600 cm^{-1}, which is assigned to the transverse optical phonon modes of GaN (Figure 1).[23−25] The absence of any trace of the gallane precursor or gallazane intermediates is additionally supported by the solid state ^{1}H-MAS NMR data of **4** (Figure S2),

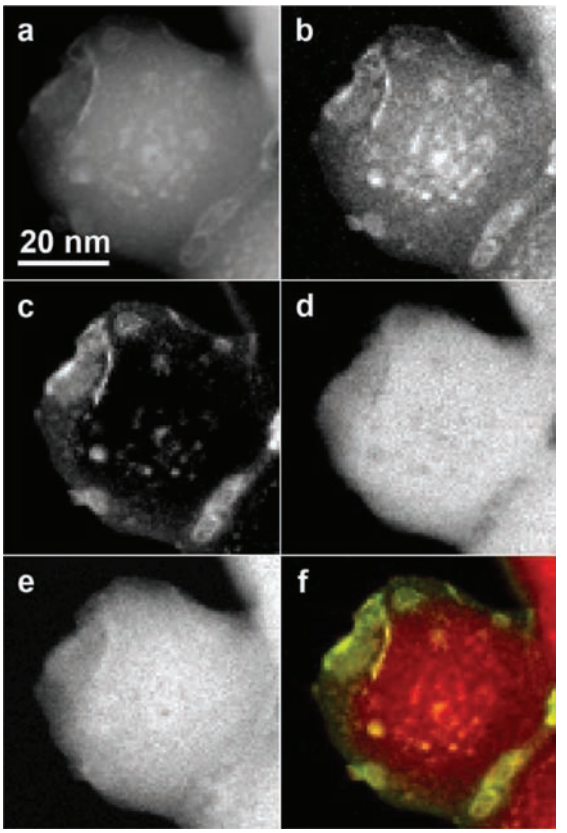

Figure 3. Elemental mapping using STEM-EELS. (a) ADF-STEM image of a GaN@ZIF-8 crystal. (b) Ga map, (c) O map, (d) N map, and (e) Zn map. (f) Color map with O in green and Ga in red.

showing only resonances for the host framework. The N_2 sorption experiments of **4** yield a specific BET surface area of 1055 $m^2 g^{-1}$ (activated ZIF-8: 1918 $m^2 g^{-1}$), indicating that pores are still very well accessible. The embedding of GaN inside ZIF-8 does not affect the overall framework stability and integrity, as seen from the TGA (Figure S1) and PXRD (Figure S4). However, diffraction peaks for crystalline GaN are not visible in the PXRD pattern of **4**, which is attributed to either very small GaN particles (<3 nm) or the relatively low amount of GaN hosted by the ZIF-8 matrix. The PXRD pattern of a physical mixture of activated ZIF-8 with microcrystalline GaN powder (13 wt % GaN) (Figure S4e) does not exhibit GaN diffraction peaks, indicating that the lacking signals of **4** might be due to low concentration.

An annular dark-field scanning transmission electron microscopy (ADF-STEM) analysis of GaN@ZIF-8 (**4**) was performed to obtain more detailed information about the location and size distribution of the embedded GaN NPs. The ADF-STEM images (Figure 2) show very small NPs (smallest particles are close to the 1.2 nm ZIF-8 cavity size) as bright dots, homogenously dispersed through the bulk of the material.[15]

Additionally, spatially resolved electron energy-loss spectroscopy (EELS) was used to map the Ga, C, N, O, and Zn distribution in a single GaN@ZIF-8 crystal (Figure 3). The Ga map shows a uniform background contrast due to the embedding of small Ga NPs throughout the ZIF-8 crystal (Figure 3b). Next to the contrast from small GaN NPs, some larger (in some cases hollow) structures can be made out in the Ga map close to the

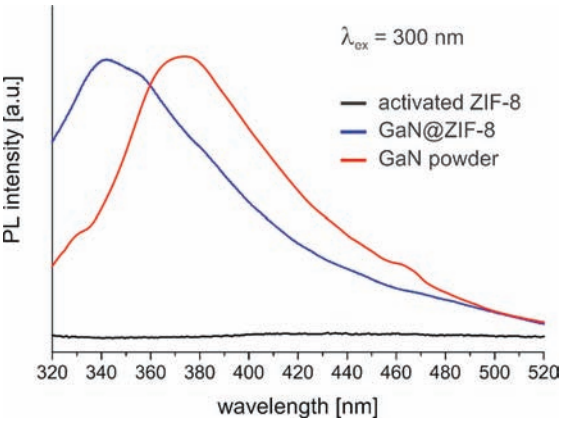

Figure 4. Room-temperature PL spectra of activated ZIF-8 (black), GaN@ZIF-8 (blue), and microcrystalline GaN powder (red), excited at 300 nm.

ZIF-8 crystal surface, which are simultaneously present in the O-map (Figure 3c). The presence of these larger (hollow) structures near the surface points to the presence of sporadic oxidized Ga, probably evoked by oxidation of clustered material at the ZIF-8 surface in air during TEM sample preparation. Note that only GaN NPs near the ZIF-8 matrix external surface are affected by this oxidation, indicating a significantly reduced reactivity of the deeper incorporated GaN NPs.

The optical properties of GaN@ZIF-8 (**4**) were examined via photoluminescence (PL) spectroscopy at room temperature. Figure 4 shows the PL spectrum of activated ZIF-8, the new composite material **4**, and microcrystalline GaN powder as a reference. A broad UV emission maximum is visible at 340 nm, which can be assigned to the near-band-gap emission of the GaN NPs, which is quite significantly shifted to higher energies compared to that of bulk GaN. This blue shift is expected for nano-sized GaN QDs and relates to the increase of the band gap in correlation to particle size (quantum-size effect). The average diameter of the embedded GaN NPs was calculated to be 2.3($\pm$0.5) nm using a simplified approach that correlates the absolute value of the energy shift (ΔE from the PL spectrum) with the QD size (Figure S8).[26]

In summary, we presented the very first example of embedding compound semiconductor quantum dots inside a metal−organic framework. Very small GaN nanoparticles are caged in the sodalite-type pore structure ZIF-8. Interestingly, the formation of GaN NPs inside the pore structure takes direct advantage of the confinement effect of the coordination space on the respective GaN precursor chemistry. The cyclotrimerization of caged $[(CH_3)_3NGaH_3]$ to yield $(H_2GaNH_2)_3$ in a quantitative and selective fashion is quite remarkable. Cyclotrigallazane has previously been shown to behave as a good precursor for GaN.[19] However, it has never been used before as an *in situ*-formed *intermediate* precursor for selective embedding GaN NPs inside the cavities of microporous matrices. Note that the obtained material GaN@ZIF-8 is still quite porous. We suggest the initial formation of Ga_3N_3 nuclei by dehydrogenation of caged cyclotrigallazane. These species may be quite mobile within the framework and eventually aggregate to GaN NPs during thermal annealing which finally occupy or affect only a fraction of the available cavities. Our results and data demonstrate the potential of materials chemistry truly *inside* MOF matrices to achieve well-defined

binary materials other than bimetallic alloys[27] or metal oxides. At this point we note the availability of the related composite ZnO@ZIF-8, which is formed by selective oxidation of [$ZnEt_2$]@ZIF-8,[7] and we suggest the possibility of combining the two approaches to eventually yield ternary solid solution-type GaN/ZnO NPs hosted by ZIFs or other suitable and chemically very robust MOF matrices, such as UiO-66.[28,29] The investigation of nanocomposite materials of this kind may be quite interesting within the context of photocatalysis, hydrogen generation, and even water splitting using visible light.

■ ASSOCIATED CONTENT

Supporting Information. Materials and methods used in the experiments, PXRD patterns, ^{13}C and ^{2}H MAS NMR spectra, and additional FT-IR, TGA, and TEM data. This material is available free of charge via the Internet at http://pubs.acs.org.

■ AUTHOR INFORMATION

Corresponding Author
roland.fischer@rub.de

■ ACKNOWLEDGMENT

This work was supported by the German Research Foundation within the Research Centre "Metal Support Interaction in Heterogeneous Catalysis" (SFB-558; fellowship for D.E. and C.W.) and the Ruhr-University Research School. S.B.K. is thankful for the financial support from the Research Department Interfacial Systems Chemistry. The authors acknowledge support from the European Union under the Framework 7 program under a contract from an Integrated Infrastructure Initiative (Ref. 262348 ESMI). G.V.T. acknowledges the ERC grant COUNTATOMS. S.T. gratefully acknowledges financial support from the Fund for Scientific Research Flanders. The microscope used in this study was partially financed by the Hercules Foundation.

■ REFERENCES

(1) Delgado-Friedrichs, O.; O'Keeffe, M.; Yaghi, O. M. *Phys. Chem. Chem. Phys.* **2007**, *9*, 1035–1043.
(2) Meilikhov, M.; Yusenko, K.; Esken, D.; Turner, S.; Van Tendeloo, G.; Fischer, R. A. *Eur. J. Inorg. Chem.* **2010**, *24*, 3701–3714.
(3) Jiang, H.-L.; Xu, Q. *Chem. Commun.* **2011**, *47*, 3351–3370.
(4) Gu, X.; Lu, Z.-H.; Jiang, H.-L.; Akita, T.; Xu, Q. *J. Am. Chem. Soc.* **2011**, *133*, 11822–11825.
(5) Cheon, Y. E.; Suh, M. P. *Angew. Chem., Int. Ed.* **2009**, *48*, 2899–2903.
(6) Suh, M. P.; Moon, H. R.; Lee, E. Y.; Jang, S. Y. *J. Am. Chem. Soc.* **2006**, *128*, 4710–4718.
(7) Esken, D.; Noei, H.; Wang, Y.; Wiktor, C.; Turner, S.; Van Tendeloo, G.; Fischer, R. A. *J. Mater. Chem.* **2011**, *21*, 5907–5915.
(8) Müller, M.; Hermes, S.; Kähler, K.; van den Berg, M. W. E.; Muhler, M.; Fischer, R. A. *Chem. Mater.* **2008**, *20*, 4576–4587.
(9) Müller, M.; Turner, S.; Lebedev, O. I.; Wang, Y.; Van Tendeloo, G.; Fischer, R. A. *Eur. J. Inorg. Chem.* **2011**, *12*, 1876–1887.
(10) White, K. A.; Chengelis, D. A.; Zeller, M.; Geib, S. J.; Szakos, J.; Petoud, S.; Rosi, N. L. *Chem. Commun.* **2009**, *30*, 4506–4508.
(11) Park, S. K.; Ni, Z.; Côté, A. P.; Choi, J. Y.; Huang, R.; Uribe-Romo, F. J.; Chae, H. K.; O'Keeffe, M.; Yaghi, O. M. *Proc. Natl. Acad. Sci. U.S.A.* **2006**, *103*, 10186–10191.
(12) Maeda, K.; Sakamoto, N.; Ikeda, T.; Ohtsuka, H.; Xiong, A.; Lu, D.; Kanehara, M.; Teranishi, T.; Domen, K. *Chem.—Eur. J.* **2010**, *16*, 7750–7759.
(13) Hafizovic, J.; Bjorgen, M.; Olsbye, U.; Dietzel, P. D. C.; Bordiga, S.; Prestipino, C.; Lamberti, C.; Lillerud, K. P. *J. Am. Chem. Soc.* **2007**, *129*, 3612–3620.
(14) Schröder, F.; Esken, D.; Cokoja, M.; van den Berg, M. W. E.; Lebedev, O. I.; Van Tendeloo, G.; Walaszek, B.; Buntkowsky, G.; Limbach, H.; Chaudret, B.; Fischer, R. A. *J. Am. Chem. Soc.* **2008**, *130*, 6119–6130.
(15) Esken, D.; Turner, S.; Lebedev, O. I.; Van Tendeloo, G.; Fischer, R. A. *Chem. Mater.* **2010**, *22*, 6393–6401.
(16) Esken, D.; Zhang, X.; Lebedev, O. I.; Schröder, F.; Fischer, R. A. *J. Mater. Chem.* **2009**, *19*, 1314–1319.
(17) Campbell, J. P.; Hwang, J.-W.; Young, V. G.; Von Dreele, R. B.; Cramer, C. J.; Gladfelter, W. L. *J. Am. Chem. Soc.* **1998**, *120*, 521–531.
(18) Jegier, J. A.; McKernan, S.; Gladfelter, W. L. *Inorg. Chem.* **1999**, *38*, 2726–2733.
(19) Jegier, J. A.; McKernan, S.; Purdy, A. P.; Gladfelter, W. L. *Chem. Mater.* **2000**, *12*, 1003–1010.
(20) Marchant, S.; Tang, C. Y.; Downs, A. J.; Greene, T. M.; Himmel, H.-J.; Parsons, S. *Dalton Trans.* **2005**, *20*, 3281–3290.
(21) Storr, A.; Penland, A. D. *J. Chem. Soc. A* **1971**, 1237–1242.
(22) Jegier, J. A.; McKernan, S.; Gladfelter, W. L. *Chem. Mater.* **1998**, *10*, 2041–2043.
(23) Bungaro, C.; Rapcewicz, K.; Bernholc, J. *Phys. Rev. B* **2000**, *61*, 6720–6725.
(24) Qiu, H.; Cao, C.; Zhu, H. *Mater. Sci. Eng., B* **2007**, *136*, 33–36.
(25) Cho, S.; Lee, J.; Park, I. Y.; Kim, S. *Mater. Sci. Eng., B* **2002**, *95*, 275–278.
(26) Madelung, O. *Semiconductors—Basic Data*; Springer: Berlin, 1996.
(27) Schröder, F.; Henke, S.; Zhang, X.; Fischer, R. A. *Eur. J. Inorg. Chem.* **2009**, *21*, 3131–3140.
(28) Cavka, J. H.; Jakobsen, S.; Olsbye, U.; Guillou, N.; Lamberti, C.; Bordiga, S.; Lillerud, K. P. *J. Am. Chem. Soc.* **2008**, *130*, 13850–13851.
(29) Gomes Silva, C.; Luz, I.; Llabrés i Xamena, F. X.; Corma, A.; García, H. *Chem.—Eur. J.* **2010**, *16*, 11133–11138.